Solar Energy Materials & Solar Cells 95 (2011) S8–S12

Contents lists available at ScienceDirect

Solar Energy Materials & Solar Cells

journal homepage: www.elsevier.com/locate/solmat

Fabrication of flexible CdTe solar modules with monolithic cell interconnection

J. Perrenoud *, B. Schaffner, S. Buecheler, A.N. Tiwari

Laboratory for Thin Films and Photovoltaics, Empa, Swiss Federal Laboratories for Materials Science and Technology, Überlandstr. 129, 8600 Dübendorf, Switzerland

ARTICLE INFO

Available online 16 December 2010

Keywords:
Polyimide
CdTe
Solar module
Monolithic interconnection
Laser scribing

ABSTRACT

CdTe solar cells and modules have been manufactured on polyimide (PI) substrates. Aluminum doped zinc oxide (ZnO:Al) was used as a transparent conductive oxide (TCO) front contact, while a thin high resistive transparent layer of intrinsic zinc oxide (i-ZnO) was used between the front contact and the CdS layer. The CdS and CdTe layers were evaporated onto the ZnO:Al/i-ZnO coated PI films in a high vacuum evaporation system followed by a $CdCl_2$ activation treatment and a Cu–Au electrical back contact deposition. In some cases prior to the cell deposition, the PI film was coated with MgF_2 on the light facing side and the effects on the optical and electrical properties of TCO and solar cells were investigated. The limitations on current density of solar cells due to optical losses in the PI substrate were estimated and compared to the experimentally achieved values. Flexible CdTe solar cells of highest efficiencies of 12.4% and 12.7% were achieved with and without anti-reflection MgF_2 coating, respectively.

Laser scribing was used for patterning of layers and monolithically interconnected flexible solar modules exhibiting 8.0% total area efficiency on 31.9 cm^2 were developed by interconnection of 11 solar cells in series.

1. Introduction

The lowest production cost per Watt achieved with CdTe solar modules on glass substrates by First Solar [1] is an indicator of the promising potential of the CdTe based solar cells. A variety of deposition methods have been used for processing CdTe solar cells [2]. Chemical robustness, ease for stoichiometry control and high growth rate (>1 μm/min) deposition possibilities are some of the attractive features of the CdTe for solar cell applications. The highest efficiency of 16.5% has been reported for CdTe solar cells developed with the close space sublimation (CSS) method on glass substrates coated with a bi-layer of stannates as transparent contact [3]. Such solar cells are processed at high substrate temperature >600 °C [4]. However, low deposition temperature (<450 °C) processes have also yielded high efficiency solar cells on glass substrates[5,6]. Such low temperature processes have also been applied for the development of flexible CdTe solar cells in substrate [7] and superstrate [8–12] configurations on polyimide (PI) films (see also review paper [13]). While the CdTe technology on glass substrates has progressed to a high level of manufacturing, the development of flexible CdTe technology has just started. The advantages of high speed deposition of CdTe/CdS and adapting those low temperature processes for roll-to-roll manufacturing could lead to reduction in production costs. Fig. 1 shows a schematic of the roll-to-roll deposition concept.

In continuation of our ongoing work on flexible CdTe solar cells we substituted ITO by ZnO:Al and achieved better performance in terms of adhesion and solar cell efficiency. The present paper discusses further studies on the development of flexible CdTe solar cells and monolithically interconnected mini-modules where laser scribing is used for patterning of the layers. In order to further improve the efficiency we analyzed the optical losses due to PI absorption and reflection and their consequences to limit the achievable current density in solar cells. The TCO resistivity and its influence on the FF of cells with different geometry were investigated in order to design a CdTe mini-module. Finally a CdTe mini-module was produced using laser scribing for patterning.

2. Experimental

CdTe/CdS solar cells in superstrate configuration were grown on PI substrates. The flexible PI films were mounted in molybdenum frames (substrate holder) to simplify the handling during processing. On some samples a 100 nm thick MgF_2 coating was applied on the light facing side of the PI film by e-beam evaporation as a first process step. Radio frequency magnetron sputtering at 300 °C substrate temperature was used for the growth of aluminum doped zinc oxide (ZnO:Al) transparent conducting oxide (TCO) front contact layer followed by a highly resistive transparent layer

* Corresponding author.
E-mail address: julian.perrenoud@empa.ch (J. Perrenoud).

0927-0248/$ - see front matter © 2010 Elsevier B.V. All rights reserved.
doi:10.1016/j.solmat.2010.11.019

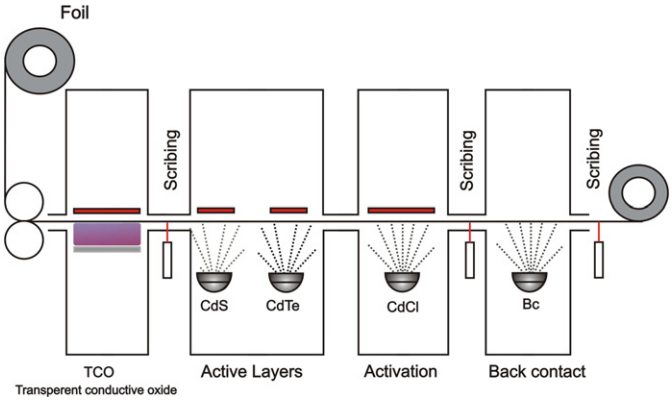

Fig. 1. Concept for CdTe module production via roll-to-roll coating.

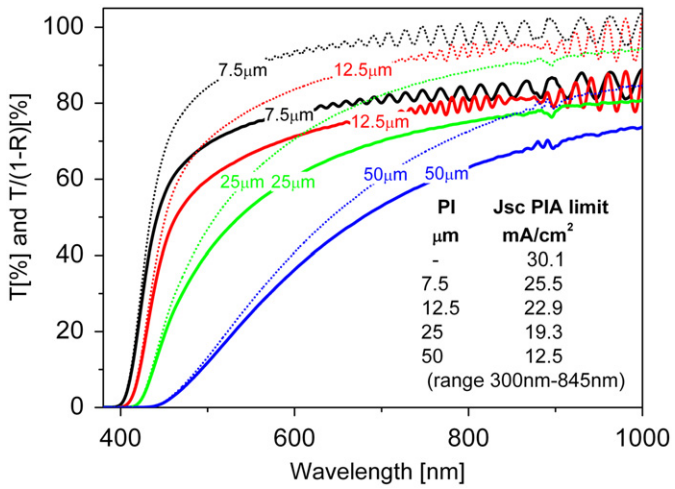

Fig. 2. Transmittance (continuous lines) and $T/(1-R)$ (dashed lines) of PI films with different thicknesses (7.5, 12.5, 25, and 50 µm, from top to bottom). The inset table shows the maximum achievable J_{sc} (J_{sc} PIA limit) for a solar cell with response from 300 to 845 nm after subtracting the photons lost due to absorption ($L_{A1}+L_{A2}$) in the PI film.

Table 1
Definition of potential J_{sc} losses caused by different optical losses in the PI film and at interfaces. T and R are the measured transmittance and reflection, respectively. $\#\gamma$ is the spectral photon irradiance according to the reference spectrum IEC 609004-4 Ed.2. A is a constant to adjust the units.

Loss name	Loss reason	Loss definition
L_{A1} (mA/cm^2)	Absorption of photons with wavelength below 400 nm in the PI	$A\int_{300}^{400}\#\gamma\, d\lambda$
L_{A2} (mA/cm^2)	Absorption of photons with wavelength above 400 nm in the PI	$A\int_{400}^{845}\#\gamma\left(1-\frac{T}{1-R}\right)d\lambda$
L_R (mA/cm^2)	Reflection loss at PI air interfaces	$A\int_{400}^{845}\#\gamma\left(\frac{T}{1-R}-T\right)d\lambda$

of intrinsic ZnO (i-ZnO). The CdS and CdTe layers were deposited by high vacuum evaporation at 165 and 350 °C substrate temperatures, respectively. The CdS layer was annealed at 420 °C for 30 min prior to CdTe deposition. The $CdCl_2$ treatment was performed by depositing 400 nm $CdCl_2$ layer on CdTe/CdS by vacuum evaporation and subsequent annealing in air at 420 °C for 20 min. The CdTe surface was etched in 0.1% diluted bromine methanol solution for 4 s and vacuum evaporated Cu/Au was applied for back electrical contact. The TCO conductivity was measured before and after solar cell processing via aluminum line contacts deposited prior to the TCO on two opposite borders of the PI substrate. The measurements of the TCO resistivity helped in optimization of processes and estimation of losses for solar module design and development. Total transmittance and reflectance measurements were performed with a Shimadzu UV 3600 spectrometer using an integrating sphere. The solar cells were characterized by current–voltage (J–V) and spectral response (SR) measurements according to the international standards IEC 60904-1 Ed.2 and IEC 60904-8 Ed2. The short circuit current density (J_{sc}) of cells and active area J_{sc} of modules under AM1.5G was calculated from EQE using the reference spectrum IEC 609004-4 Ed.2.

3. Results and discussions

3.1. Polyimide absorption and resulting J_{sc} limitation

Since light passes through the PI substrate in CdTe solar cells in superstrate configuration an optical loss occurs due to absorption in the PI and reflection at the interfaces. We have investigated optical properties of PI of different thicknesses used in the development of flexible solar cells. The total transmittance T and total reflection R of the PI films with different thicknesses (7.5, 12.5, 25, and 50 µm) were measured. Three losses were defined as shown in Table 1. These definitions were chosen as they lead to a realistically achievable current density (J_{sc}) potential analysis. They are based on the simplified model $T(\lambda)=(1-R(\lambda))e^{-\alpha(\lambda)x}$ where $T(\lambda)$ is the measured transmittance, $R(\lambda)$ the measured reflectance, $\alpha(\lambda)$ the absorption coefficient, and x the PI thickness. The transmittance (T) and 1 − absorption ($T/(1-R)$) spectra for PI films (uncoated) of different thicknesses are shown in Fig. 2. The absorption coefficient of the PI was found to be 5×10^3 cm^{-1} in the range between 300 and 400 nm as determined from T and R measurements following the simplified model mentioned above.

Due to the high absorption coefficient of the PI, the photons below 400 nm are completely absorbed already in the thinnest PI investigated (7.5 µm). This fact is represented by the loss L_{A1}, which is 1.3 mA/cm^2 for all investigated PI thicknesses. The loss L_{A2} represents the thickness dependent absorption loss of photons with wavelengths between 400 and 845 nm in the PI. It is defined via the expression $T/(1-R)$ and results in a potential J_{sc} loss of 3.3, 5.9, 9.5, and 16.2 mA/cm^2 for the investigated PI thicknesses of 7.5, 12.5, 25, and 50 µm, respectively. The loss L_R represents the reflection loss and was defined via the measured reflectance weighed with the absorption probability for the specific wavelength ($Re^{-\alpha x}=T/(1-R)-T$). Such defined reflection loss was found to be 4.2, 3.4, 2.8, and 1.5 mA/cm^2 for the 7.5, 12.5, 25, and 50 µm PI, respectively.

There are ways to reduce all three above mentioned losses (L_{A1}, L_{A2}, L_R). The reflection loss can be reduced by applying an anti-reflection coating on the light facing side of the PI and might be reduced by the ZnO on the backside. The absorption losses L_{A1} and L_{A2} could be reduced via the luminescent down-shifting [14]. As the flexible CdTe device on PI would require encapsulation on both sides, there is a natural place to put a luminescent dye, e.g., in the encapsulation film (if used) or the encapsulant. With luminescent down shifting the CdS absorption loss could be reduced in the same step [15] giving an additional benefit. As there are strategies to reduce all three optical losses, and the development of more transparent PI is in progress, the achievable J_{sc} limits can be higher in future flexible solar modules than estimated in this work at present. For the cells and modules discussed in this work the PI absorption ($L_{A1}+L_{A2}$) limits the maximum achievable J_{sc}. This restriction by the PI absorption losses (30.1 mA/cm^{-2} $L_{A1}-L_{A2}$) will be denoted as the J_{sc} polyimide absorption limit (**J_{sc} PIA limit)** in the following (see inset table of Fig. 2).

3.2. Solar cell properties

Solar cells of size from 0.15 up to 2.9 cm^2 were grown on PI films of different thicknesses. Using ZnO:Al as TCO combined with i-ZnO as highly resistive and transparent (HRT) layer higher efficiency (η=12.4%, V_{oc}=823 mV, J_{sc}=19.6 mA/cm^2, FF=76.5%) solar cells were obtained compared to the cells with ITO/i-ZnO (V_{oc}=765 mV, J_{sc}=20.9 mA/cm^2, FF=71%) [9,11,12]. The use of ZnO:Al leads to excellent adhesion and significantly lower stress compared to ITO.

The ZnO:Al on PI showed a higher sheet resistance (> 10 $\Omega_\square$) compared to layers on glass (5 $\Omega_\square$) deposited under the same sputter conditions. This is surprising as Herrero and Guillén [16] have reported that in case of ITO, with proper optimization layers lower resistivity compared to glass can be achieved on PI film. Furthermore, a degradation of conductivity was observed when TCOs were measured in the finished device. Degassing of the PI and subsequent coating with a multifunctional 100 nm thick MgF_2 layer on the light facing side reduced the initial difference of the sheet resistance between ZnO:Al on glass and PI. In addition the degradation of conductivity was also reduced with this procedure as illustrated in Fig. 3. The sheet resistance of TCOs in finished, non-encapsulated samples is shown as a function of storage time in ambient air. The initial difference in TCO conductivity between cells with and without MgF_2 can be explained by protection of the TCO by the chemically robust MgF_2 (PI is to some extent permeable for water vapor [17] and oxygen). Vasko et al. [18] observed an increase in the sheet resistance of ZnO:Al during the $CdCl_2$ treatment (uncovered layer). Further the resistance of ZnO:Al is known to increase by air annealing due to the absorption of oxygen [19]. Mechanical stress due to excessive bending can also lead to increase in the resistance of the TCO layers.

The CdS layer thickness was optimized and maximum efficiency was achieved with a thickness of 120 nm. The optimum value is shifted towards thicker CdS compared to the cells on glass due to the coincidence of strong PI absorption in the wavelength region where the CdS absorption loss occurs (optimum thickness on glass 60–90 nm [5]). The CdTe thickness did not show a significant effect on the cell parameters when varied between 4 and 6 μm.

With the optimization of various process parameters till now solar cells with efficiency up to 12.4% were produced on 7.5 μm PI without anti-reflection coating [11]. A summary of some flexible solar cells at different PI thicknesses is given in Table 2. Solar cells

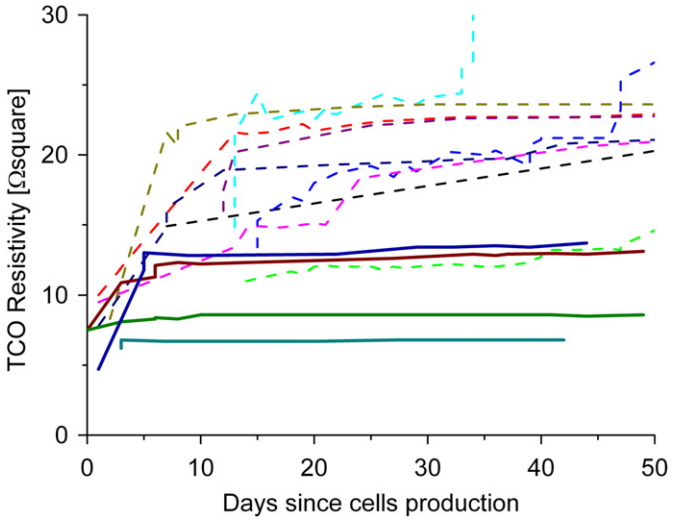

Fig. 3. TCO resistivity of finished and non-encapsulated cells on PI with (straight lines) and without (dotted lines) MgF_2 coating. The resistivity of TCOs grown on MgF_2 coated PI is lower and more stable.

Table 2
J–V parameters of some high efficiency cells on PI films of different thicknesses. J_{sc} decreases with increasing PI thickness, as predicted from optical loss analysis. J_{sc}/J_{sc} PIA limit is the experimentally achieved J_{sc} divided by the calculated J_{sc} PIA limit value (see Fig. 2 inset table). For example J_{sc}/J_{sc} PIA limit=85% means that in addition to the PI absorption losses 15% of the photons were lost due to other loss mechanisms like reflection, recombination, and absorption in the CdS.

PI (μm)	V_{oc} (mV)	J_{sc} (mA/cm^2)	$\frac{J_{sc}}{J_{sc}\ \text{PIA limit}}$ (%)	**FF** (%)	η (%)
7.5 [a]	823	19.6	77	76.5	12.4
7.5	803	21.6	85	73.5	12.7
12.5	799	19.8	86	72.2	11.4
25	826	16.7	87	69.3	9.6

[a] No anti-reflection coating.

Table 3
J–V parameters of solar cells on 7.5 μm thin PI with different cell geometry.

Size (cm^2)	V_{oc} (mV)	**FF** (%)	J_{sc} (mA/cm^2)	η (%)
0.5 × 0.3	803	**73.5**	21.6	12.7
0.5 × 0.5	799	**69.2**	19.6 [a]	10.8 [a]
1.0 × 0.5	819	**64.4**	22.0	11.6
2.0 × 0.5	811	**61.9**	22.0	11.1
5.8 × 0.5	805	**60.4**	21.6	10.5
1.0 × 1.0	755	**51.7**	19.4 [a]	7.6[a]

[a] No anti-reflection coating.

on MgF_2 coated PI reached about 85% of the J_{sc} PIA limit. Hence, the sum of all additional losses to the PI absorption, such as remaining reflection, TCO free carrier absorption, CdS absorption, and recombination is 15% of all photons. The J_{sc} difference between cells on MgF_2 coated and uncoated PI can be explained by reduced reflectance. To quantify the J_{sc} gain, the reflectance of finished devices with and without MgF_2 coating was measured. The average reflection of a cell at 7.5 μm PI without anti-reflective coating was found to be 12.0% in the range of 400–845 nm. The average reflection of the bare PI in the same wavelength range was 16.3%. Hence it can be concluded that the solar cell structure on the backside reduced the reflection by 4.3% absolute. After applying an anti-reflective coating on the light facing side the average cell reflection dropped to 3%. The difference in reflectance between cells with and without MgF_2 is expected to yield a gain in J_{sc} of 1.8 ± 0.1 mA/cm^2 calculated taking the spectral irradiance, internal quantum efficiency of the cells, and absorption of the PI into account. On average, cells with MgF_2 coating showed an increased J_{sc} of 1.7 ± 0.3 mA/cm^2 compared to cells on uncoated PI. The fact that J_{sc} gain calculated out of reflection measurement and EQE measurements agree means that a significant influence of the MgF_2 on changes of other optical properties can be excluded (e.g. darkening during the $CdCl_2$ treatment).

With the intention to produce flexible solar modules the solar cell size was scaled up to analyze the losses. A decrease in efficiency was observed with increasing cell size (Table 3), which was mainly caused by a lower fill factor (FF). The main reason for the FF drop is the limited TCO conductivity as derived in the following.

For a rectangular cell with width L (defined as shorter side), and TCO sheet resistance $\rho_s[\Omega_\square]$, the FF depends on the parameter $\delta = \rho_s L^2 J_{sc}/V_{oc}$ [20]. The FF drop due to power loss in the TCO can be estimated using the following equation [20]:

$$\frac{FF}{FF_o} = 1 - 0.37\delta \quad (1)$$

FF_o is the fill factor of an infinitely small cell (or a cell with ρ_s=0). Taking the dimension of the cell and a sheet resistance of ρ_s=15 $\Omega_\square$ the calculated fill factor drop is comparable to the

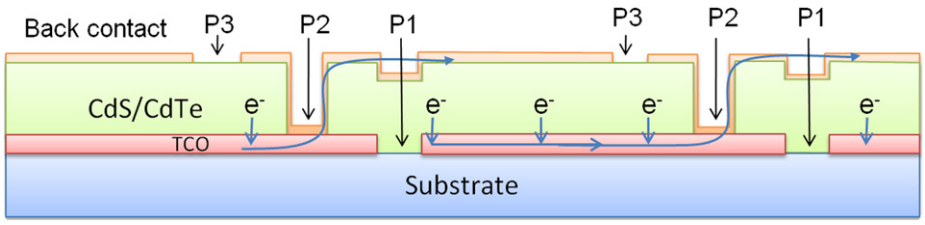

Fig. 4. Schematic of the monolithically interconnected flexible CdTe solar module.

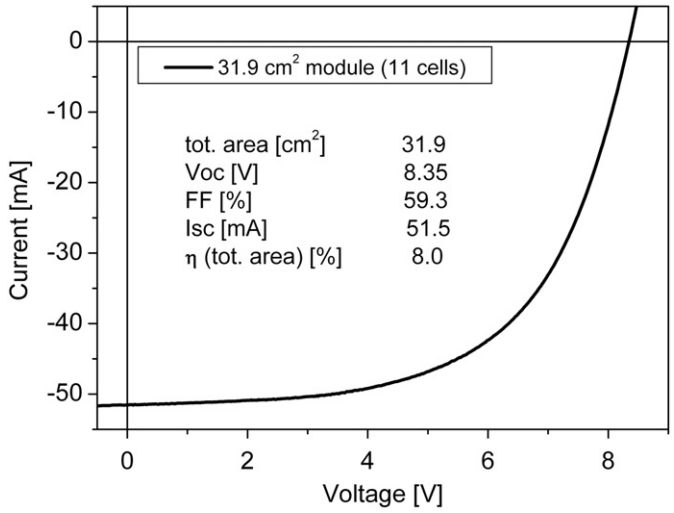

Fig. 5. *I–V* characteristics of a monolithically interconnected flexible module.

experimentally observed values. Based on the experimental results and the FF loss estimation a solar cell width of 0.5 cm was chosen for the monolithically interconnected flexible solar module development.

3.3. Flexible solar modules

Earlier preliminary attempts to produce monolithically interconnected flexible CdTe modules using shadow mask methods yielded 3.5% efficiency [10]. In the work presented here laser scribing was used for patterning of layers on PI films. After the TCO deposition (ZnO:Al and i-ZnO) the TCO was scribed to separate the front contact (P1 scribe). After the CdS/CdTe deposition and subsequent treatment the CdS/CdTe was removed to enable a contact from front to the back contact (P2). Finally, after the back contact deposition the cells were separated by the third scribe (P3).

A schematic cross-section of the monolithically interconnected solar modules is shown in Fig. 4. According to the above mentioned estimations (see Table 3 and Eq. (1)) a cell width of 0.5 cm was chosen. The length was 5.8 cm and 11 cells were electrically interconnected in series. The loss of active area due to dead interconnection zones was 15%. The resulting *I–V* curve is shown in Fig. 5.

The active area J_{sc} of the module was determined via measuring EQE of the single cells and calculating the average value. An average value of 20.9 mA/cm^2 was found with a standard deviation of 0.8 mA/cm^2. The total area and active area efficiency of the solar mini-module is 8.0% and 9.4%, respectively.

4. Conclusion

The J_{sc} of solar cells is limited by the absorption of the PI film and the reflection at the PI air interface. Application of an anti-reflection coating reduced the average reflection of the solar cell in the range of 400–845 nm from 12% to 3% which translates into a J_{sc} gain of 1.7 mA/cm^2. The thickness dependent absorption loss in the PI film restricts the J_{sc} values, e.g., to 25.5 mA/cm^2 for 7.5 μm and 12.5 mA/cm^2 for 50 μm thin PI film. The TCO conductivity was identified as limiting factor for the FF of large (0.5 cm^2 and larger) cells.

Using ZnO:Al as TCO and MgF_2 as anti-reflection coating 12.7% efficient flexible solar cells were achieved. Laser patterning technique was implemented to develop 8% efficient monolithically interconnected solar modules. Further improvements in module efficiency could be expected by reducing the width of the scribe lines and increasing the conductivity of the TCO layer.

4.1. Prospects and technological issues

Due to roll-to-roll process ability flexible CdTe solar cells are promising candidates for low cost solar module manufacturing. As for inline production a polyimide thickness of 25 μm is preferable to provide sufficient mechanical stability in the roll-to-roll coating system; the optical absorption in the PI film is a major limiting factor for module efficiency. There are three approaches to reduce or avoid this absorption loss. One is to apply more transparent PI; the second approach is to integrate luminescent down shifting and the third to grow the CdTe solar cells in substrate configuration.

Application of high mobility TCOs [21] will have only little scope for improvement while the deposition at high temperature could be a problem. The application of a long term stable back contact on the flexible solar cells remains to be implemented. We have successfully increased the growth rate of CdTe to 0.5 μm/min with no efficiency loss [22]. The roll-to-roll manufacturability still remains to be demonstrated since we do not have roll-to-roll coating machines available in our laboratories.

Acknowledgement

We would like to thank the company FLISOM AG, for performing the laser scribing and helping in the mini-module development.

References

[1] First Solar web page. 〈www.firstsolar.com〉, 2010.
[2] N. Romeo, A. Bosio, V. Canevari, A. Podestà, Recent progress on CdTe/CdS thin film solar cells, Sol. Energy 77 (2004) 795–801.
[3] X. Wu, J.C. Keane, R.G. Dhere,C. DeHart, D.S. Albin, A.Duda, T.A.Gessert, S. Asher, D.H. Levi, P. Sheldon, 16.5%-efficient CdS/CdTe polycrystalline thin film solar cell, in: Proceedings of the 17th European Photovoltaic Solar Energy Conference, Munich, Germany, 2001, pp. 995-1000.
[4] X. Wu, High-efficiency polycrystalline CdTe thin-film solar cells, Sol. Energy 77 (2004) 803–814.
[5] J. Perrenoud, L. Kranz, S. Buecheler, F. Pianezzi, A.N.Tiwari, The use of aluminum doped ZnO as transperent conductive oxide for CdS/CdTe solar cells, Thin Solid Films, in preparation.
[6] A. Gupta, A.D. Compaan, All-sputtered 14% CdS/CdTe thin-film solar cell with ZnO:Al transparent conducting oxide, Appl. Phys. Lett. 85 (2004) 684–686.
[7] J.P. Enríquez, X. Mathew, G.P. Hernández, U. Pal, C. Magaña, D.R. Acosta, R. Guardian, J.A. Toledo, G. Contreras Puente, J.A. Chávez Carvayar, CdTe/CdS solar cells on flexible molybdenum substrates, Sol. Energy Mater. Sol. Cells 82 (2004) 307–314.

[8] A. Romeo, H. Zogg, A.N. Tiwari, Influence of proton irradiation and development of flexible CdTe solar cells on polyimide, in: MRS Proceedings, vol. 668, 2001, H3.3.1.
[9] A. Romeo, G. Khrypunov, F. Kurdesau, M. Arnold, D.L. Bätzner, H. Zogg, A.N. Tiwari, High-efficiency flexible CdTe solar cells on polymer substrates, Sol. Energy Mater. Sol. Cells 90 (2006) 3407–3415.
[10] G. Khrypunov, A. Romeo, F. Kurdesau, D.L. Bätzner, H. Zogg, A.N. Tiwari, Recent developments in evaporated CdTe solar cells, Sol. Energy Mater. Sol. Cells 90 (2006) 664–677.
[11] J. Perrenoud, S. Buecheler, A.N. Tiwari, Flexible CdTe solar cells and modules: challenges and prospects, in: Proceedings of the SPIE, vol. 7409, 2009, pp. 74090L-1–74090L-5.
[12] J. Perrenoud, S. Buecheler, A.N. Tiwari, Flexible CdTe solar cells with high photovoltaic conversion efficiency, in: Proceedings of PVSC, 34th IEEE 2009, pp. 695–699.
[13] X. Mathew, J.P. Enriquez, A. Romeo, A.N. Tiwari, CdTe/CdS solar cells on flexible substrates, Sol. Energy 77 (2004) 831–838.
[14] E. Klampaftis, D. Ross, K.R. McIntosh, B.S. Richards, Enhancing the performance of solar cells via luminescent down-shifting of the incident spectrum: a review, Sol. Energy Mater. Sol. Cells 93 (2009) 1182–1194.
[15] T. Maruyama, R. Kitamura, Transformations of the wavelength of the light incident upon CdS/CdTe solar cells, Sol. Energy Mater. Sol. Cells 69 (2001) 61–68.
[16] J. Herrero, C. Guillén, Transparent films on polymers for photovoltaic applications, Vacuum 67 (2002) 611–616.
[17] E. Sacher, J.R. Susko, Water permeation of polymer films. I. Polyimide, J. Appl. Polym. Sci. 23 (1979) 2355–2364.
[18] A.C. Vasco, X. Liu, A.D. Compaan, All-sputtered CdS/CdTe solar cells on polyimide, in: Proceedings of PVSC, 34th IEEE Philadelphia, 2009, pp. 001552–001555.
[19] P. Nunes, E. Fortunato, R. Martins, Influence of the post-treatment on the properties of ZnO thin films, Thin Solid Films 383 (2001) 277–280.
[20] G.T. Koishiyev, J.R. Sites, Impact of sheet resistance on 2-D modeling of thin-film solar cells, Sol. Energy Mater. Sol. Cells 93 (2009) 350–354.
[21] S. Calnan, A.N. Tiwari, High mobility transparent conducting oxides for thin film solar cells, Thin Solid Films 518 (2010) 1839–1849.
[22] In preparation..